ELSEVIER

Journal of Arid Environments 72 (2008) 411–422

Journal of Arid Environments

www.elsevier.com/locate/jaridenv

Sand dune activity in north-eastern Patagonia

H.F. del Valle*, C.M. Rostagno, F.R. Coronato, P.J. Bouza, P.D. Blanco

CENPAT (CONICET), C.C. 128, (9120) Puerto Madryn (Chubut), Argentina

Received 7 March 2006; received in revised form 18 July 2007; accepted 20 July 2007
Available online 4 September 2007

Abstract

The Valdes Peninsula has the most noticeable aeolian landforms of the Patagonian drylands. The southern sector of the peninsula is affected by the advance of several fronts of active sand dunes grouped in discrete megapatches. The objectives of the study were to: (1) analyse the morphology of sand dunes, and (2) measure the migration rates and orientation of the sand dunes along a 33-year period (1969–2002). These studies used a series of field techniques in conjunction with aerial photography and satellite data, such as AVIRIS and Landsat imagery. Four main types of active sand dune forms were identified: (1) compound linear; (2) compound transverse; (3) compound dome-shaped; and (4) complex dome-shaped. Because of the windy climate, dune mobility is high; there is an eastward migration to an average speed of $9.1 \pm 2.7\,\mathrm{m\,yr^{-1}}$. Despite this high rate and since observed changes in the total area of active dunes were small, active processes of vegetation encroachment are deducible. Thus, wind and effective rainfall appear as the main factors regulating the process, in short and long-term, respectively. Although the orientation and disposition of the dunefields is in agreement with the prevailing west winds, the active dunes present a variety of forms, which reflect local variations in the wind flow. The circulation is strongly influenced by the shape of the coastline and the actual existence of the dunefields is due to this friable windward coast found nowhere else in Patagonia.

Keywords: Argentina; Coastal dunefield; Dune mobility; Remote sensing; Wind regime

1. Introduction

The Valdes Peninsula (Chubut province, north-eastern Patagonia, Argentina) has the most noticeable aeolian landforms of the Patagonian drylands. The southern sector of the peninsula is affected by the advance of several fronts of active sand dunes grouped in discrete megapatches, which are moving at different distances from the western coast, where they were generated. Although the dunes currently active represent the largest area affected by wind erosion and deposition in the whole of Patagonia, information on their characteristics and dynamics is still scarce. The largest active dune megapatch fronts clearly represent a geologic process occurring since the upper Pleistocene or early Holocene at least (Haller et al., 2000); however, some small dune megapatch fronts seem to have been originated from blowouts in post-settlement times less than 100 years ago (Blanco, 2004).

*Corresponding author. Tel.: +54 2965 451024x326; fax: +54 2965 451543.
E-mail address: delvalle@cenpat.edu.ar (H.F. del Valle).

0140-1963/$ - see front matter © 2007 Elsevier Ltd. All rights reserved.
doi:10.1016/j.jaridenv.2007.07.011

The sources of sediment are the sandy beaches of Nuevo Gulf where a continued supply of loose, sand-sized sediment is available to be transported inland by the prevailing westerly winds (Haller et al., 2000). Sand is also derived from weathering and erosion of tertiary marine sediments (sandstones and mudstones) in the cliffs on the shoreline. The relic aeolian forms that are found in the coastal section lying over old abrasion platforms are currently being eroded by the sea (Súnico, 1996). Therefore, the material detached from the western coast adopts an eastward movement and forms sand dunes, which eventually reach the Atlantic open coast after crossing the peninsula.

Evidences indicating that dune activity has been both more extensive and intense in the past occur throughout the Valdes aeolian geomorphic system. These include a series of forms stabilised by vegetation as dune systems, relic climbing and falling dunes (sand ramps), and discontinuous sand mantles in gravel plains (Bouza et al., 2005; Súnico, 1996); other evidences are the sand mantles stabilised on beach ridges (Bouza et al., 2002).

Remote sensing techniques have been applied to identify and characterise sand dunes and their temporal dynamism (Collado et al., 2002; Janke, 2002; Marin et al., 2005; Paisley et al., 1991). The use of remote sensing in the Valdes Peninsula provides a regional perspective allowing clear identification of the sand accumulated along discrete paths of transport. In a windy region such as eastern Patagonia and because of the shape of the shoreline, the uniqueness of the west (windward) coast of the Valdes Peninsula makes the dunefields of this area a good example of coastal dunes migrating inland. The aims of the study were to: (1) analyse the morphology of sand dunes in relation to the wind patterns, and (2) measure the migration rates and orientation of the sand dunes along a 33-year period (1969–2002).

2. Materials and methods

2.1. Study site

The Valdes Peninsula is on the east coast of Patagonia (42°05′–42°53′S and 63°30′–64°37′W). It is surrounded by the San Matías Gulf to the north; the San José Gulf to the north-west; the Nuevo Gulf to the south-west; and the Atlantic Ocean to the east and south. Observations on the spatial arrangement mostly of active sand dunes types were conducted in an area of 1231 km^2 centred at 42°43′S, 63°57′W (Fig. 1).

The climate is temperate and arid (13 °C and 231 mm, annual averages 1912–2002). Marine influences are much stronger in the local climate when compared to the adjacent mainland, especially in reducing the

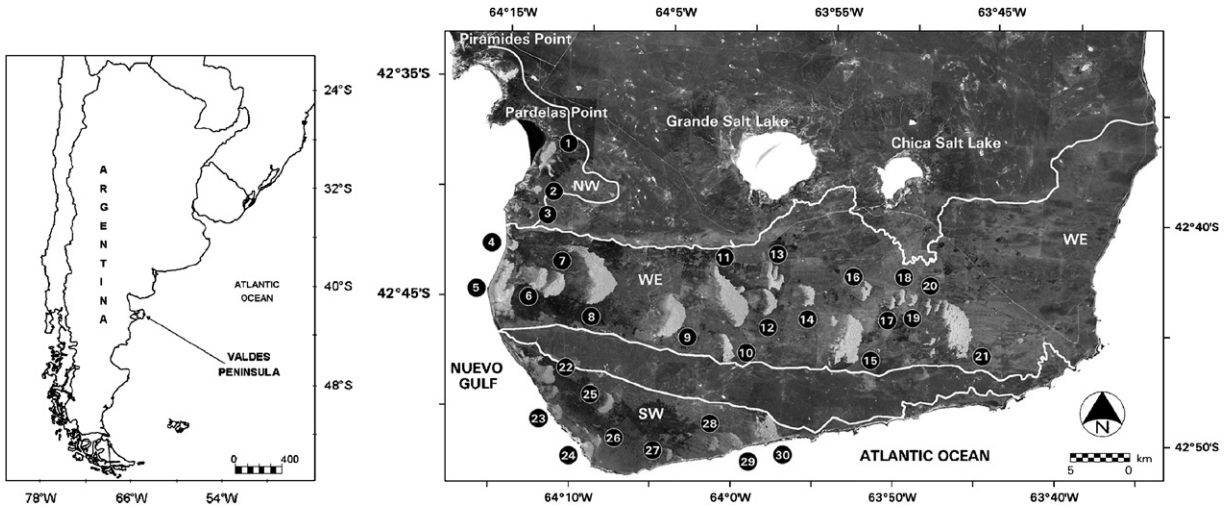

Fig. 1. Valdes Peninsula dunefields with representative dune crest and active sand dune megapatches. NW: coastal north–west dunefield; WE: west to east fringe dunefield; SW: south-west corner dunefield. The 30 active sand dune discrete megapatches studied are also shown (Landsat 7 ETM+, panchromatic band, 7th February, 2002).

temperature annual range (10.6 °C versus 14.0 °C), the number of days of frost (<20 versus 40) and interannual rainfall fluctuations (coefficient of variation = 30% versus 44%). Although a definite rainy season is lacking in the area, rainfall is more frequent in autumn and winter, so aridity conditions are clearly tempered during this semester. The Valdes Peninsula shares with the rest of Patagonia the same windy conditions (annual mean wind speed $>4.0\,m\,s^{-1}$), but the predominance of westerly winds is less important here, as north and north-east winds become more frequent according to its eastern position and more influenced by the SW Atlantic anticyclone (Paruelo et al., 1998).

Gravel deposits locally named "Rodados Patagónicos" in part cover the Valdes Peninsula (Pliocene–Pleistocene age). Older geologic units are exposed in the littoral cliffs and in the erosion fronts of tectonic depressions; they consist mainly of Tertiary marine sediments (Miocene age). The study area is characteristic of the gravel plains and sand deposits (Haller et al., 2000).

The vegetation is transitional between the southern portion of the Monte Phytogeographic Province and the northern portion of the Patagonian Province (León et al., 1998). In the study area most widespread communities are: (i) grass steppe of *Sporobolus rigens* and *Stipa tenuis*, (ii) mosaic of grass steppe of *S. rigens* and *S. tenuis* and scrub steppe of *Hyalis argentea*, (iii) grass steppe of *Piptochaetium napostaense*, *S. tenuis* and *Plantago patagonica*, (iv) mosaic of grass steppe of *P. napostaense*, *S. tenuis* and *P. patagonica* and shrub-grass steppe of *Chuquiraga avellanedae* and *S. tenuis*. The vegetation cover is 60–80% on the vegetated dunes.

Destabilisation of dune vegetation because of grazing seems to be a problem at present (Blanco, 2004). Sheep raising, mainly for wool production, is the main land use type of the Valdes Peninsula rangelands. Sheep were introduced into the area at the beginning of the last century and are presently raised in large farms (5000–10000 ha) consisting of several paddocks around shared water points.

2.2. Climatic data

In the Valdes Peninsula, the only available records on wind direction are those of Punta Delgada station, operating in the period 1959–1968. To overcome this lack and to place the study area within a wider regional context, average annual wind speed and frequency records from the following meteorological stations also were taken into account: Viedma (1951–1966 and 1971–1980), San Antonio (1961–1980), Puerto Madryn (1982–2002), Trelew (1961–2002), Cabo Raso (1961–1980) and Camarones (1971–1980), all of them gathered from the CENPAT (CONICET) climatic database. Besides, next offshore wind data were taken from Wind Atlas for ERS 1-2 satellites from November 1991 to May 2002 for two points (A and B) located over the 42°30′S parallel, at 62°30′W and 63°30′W, respectively (http://www.ifremer.fr/cersat/fr/data).

To assess regional wind intensity (WI), defined as wind speed ($m\,s^{-1}$) × frequency, the vector sum and direction of winds were calculated for each one of the above stations. Further analysis was performed with the records of Punta Delgada, the closest station to the study site, from which monthly means of wind speed and direction were available. Regional wind drift potential (DP) was estimated by means of the Fryberger model (Fryberger, 1979) with wind data aggregated into the usual 8 compass directions (45° wide bins). Vector analysis was used to determine the resultant drift direction (RDD) and the resultant drift potential (RDP).

Puerto Madryn station, 80-km westward of the study area, furnished monthly average data of wind speed and temperature (1982–2002). To extend the wind record throughout the study period starting in 1960, data previous to 1982 were calculated from the Trelew INTA station (1969–2002 series; 120-km south-west of the study area). To test the accuracy of this extrapolation, both series were correlated within the 1991–2002 period, resulting in a coefficient $r^2 = 0.61$ ($p < 0.05$).

To calculate the dune mobility index (Lancaster, 1988), the nearest available monthly data were employed, that is Puerto Madryn station for wind speed and temperature and La Adela ranch (1912–2002), 30 km from the study area for rainfall. The Lancaster model for dune mobility reads: $M = W/(P/PET)$, where M is the mobility index, W is the percentage of time during which wind speed is higher than $4.5\,m\,s^{-1}$ (at a height of 1-m), P is the precipitation value ($mm\,month^{-1}$), and PET is the potential evapo-transpiration (mm/month) estimated according to Thornthwaite and Mather (1957). Dunes are categorised as *inactive* when M values are below 50, *crest active* when values lie between 50 and 100, *flank active* when M values are between 100 and 200 and *fully active* when M values exceed 200.

A shorter series (1994–2000) of hourly data of wind speed was available in Cracker station (50-km away the study area) but it was just used to assess the percentage of time during which wind speed exceeded the threshold defined by Lancaster (1988). A straight linear correlation exists between hourly average wind speed and percentage above the threshold ($r^2 = 0.99$, $p < 0.05$). The goodness of fit allowed calculating the same percentage to monthly average wind speed data.

2.3. Remote sensing data

Changes in size, shape and position of sand dune megapatches were monitored using digital air photos and Landsat images (Table 1). The aerial photographs were scanned at a resolution of 600 dpi (binary 8 bit/byte integers, digital values: 0–255) and converted to tagged interchange format (TIFF) for use in Erdas Imagine software (ERDAS Inc., 2003). A block bundle adjustment was performed to determine the necessary information required for rectification, including the position and orientation of each image. The approach developed for this procedure was based on the selection of a master IGM photograph. Images were georeferenced by collecting ground control points (GCPs) from fieldwork and available IGM digital orthoquarterquads.

Field collection of 200 GCPs was conducted throughout the south Valdes Peninsula during the period of 1999–2002. The study area was also calibrated using 50 geodesic points from the National Geodesic Network to anchor the surveys to the existent images and maps. Control points were installed in the field to check the accuracy of the sand dune mobility observations. All images were projected into Transverse Mercator with WGS 1984 spheroid and datum. Each image was registered using a first-order polynomial and nearest neighbour resampling. Spatial resolution was 2-m and then a mosaic was made. Errors in location on this product are approximately less than one pixel size on the average. The mosaic resolution was degraded to 30-m to match multispectral data.

Landsat images were referenced to the aerial photographs mosaic to produce higher accuracy transformations (Bannari et al., 1995). The criteria for accepting a transformation for Landsat images included: (a) total root mean square (RMS) error less than 15-m (<0.5 pixel); (b) uniform geometry of GCPs; and (c) inclusion of the maximum number of GCPs that met the total RMS error criteria. The panchromatic and multispectral band pixel of different sizes (Landsat 7 ETM+) were co-aligned by assigning nominal pixel sizes of 0.5 and 1, respectively, so that the geometric transformation calculated for the panchromatic band could be applied to all bands and enable larger scales to be used. The position of GCPs in Landsat 7 ETM+ image was plotted using a false colour composition RGB, bands 5, 8 and 2 (mid-infrared, panchromatic and green, respectively). Both thermal bands (TM and ETM+) were excluded.

The range wavelength (841 nm) from the Airborne Visible/IR Image Spectrometer (AVIRIS) data was used to visualise some dune morphological features digitally. The NASA AVIRIS images were taken on June 15, 2001. The aircraft collected data at a spatial resolution of 3.4-m per pixel at low altitude. The data were radiometrically calibrated at the AVIRIS data facility (Jet Propulsion Laboratory, Pasadena, CA).

Table 1
Aerial photographs and Landsat imagery analysed in this study. Scene centre is 42°43′S, 63°57′W

Sensor	Media	Acquisition date	Distributor
Aerial photograph	Paper print (scale 1:60000)	07/01/1969	IGM[a]
Aerial photograph	Paper print (scale 1:20000)[b]	01/01/1970	SHN[c]
Landsat 5 TM		02/11/1986	USGS[d]
Landsat 7 ETM+	Digital product, CD ROM	07/02/2002	CONAE[e]

[a]Instituto Geográfico Militar.
[b]Coastal areas (discontinuous cover). These data were used only to characterize some dune morphologies.
[c]Servicio de Hidrografía Naval.
[d]U.S. Geological Survey, Sioux Falls, South Dakota. Orthorectified image.
[e]Comisión Nacional de Actividades Espaciales or the Argentinean Space Agency (level-1 data).

2.4. Dune measurements

The active dune types were classified according to morphological criteria of Bishop et al. (2002). The combination of individual dunes (compound and complex) followed McKee (1979). Sand bodies that have no identifiable mounds were designated as sand sheets.

For the assessment of sand dune mobility, we selected 30 active sand dune megapatches, out of 42 existing in the study area. In order to normalise the range of grey and colour levels among aerial photographs and Landsat images, respectively, relative radiometric calibrations were performed in Erdas 8.7 (ERDAS Inc., 2003) by matching the histograms. The calibrated photos and images were then classified using a supervised classification scheme with a maximum likelihood classifier. Two classes were defined: (1) bare sand, and (2) vegetation. The classified images were rescaled to 1 bit (1: sand and 0: vegetation).

Raster sand dune megapatches were vectorised; in all cases, the vectorisation was checked and refined by overlaying the aerial photos and Landsat images successively. Three operations were performed upon the output vector polygons: (1) removal of unwanted polygons, (2) vector cleaning to fix broken polygons, and (3) building of vector topology.

According to Levin and Ben-Dor (2004), we used the following steps for determining sand dune megapatch movement rate: (a) the lines representing the sand dune megapatch front in the years 1969, 1986 and 2002 are joined, forming a polygon, which represents the area covered by sand during those years; (b) for each polygon, the length of the sand dune megapatch moving front is automatically extracted as the skeleton line, using a vectorising technique (Peuquet, 1981); (c) the advance rate of a sand dune megapatch is then calculated as follows: $v = S/t/L$, where v is the movement rate, S the area covered by sand between successive years, t is the time between successive remote sensing data and L is the sand dune megapatch front length.

3. Results

3.1. Regional and local wind patterns

The annual values of wind intensity in north-eastern Patagonia are shown in Fig. 2a. The vector sum and direction of winds were calculated for each one of the mapped stations. The resulting wind drift potential (RDP) vectors in Punta Delgada station are shown in Fig. 2b–c. In annual values (Fig. 2b), Punta Delgada shows a clear bi-directional pattern in which the high prevalence of N wind is not found elsewhere in Patagonia. Otherwise, the importance of SW wind is far from uncommon in the region, and shared with Puerto Madryn, the second closest station to the study area. Yearly resulting drift direction (RDD) is WNW–ESE, azimuth 98°, fairly in agreement with the direction of the displacement of most of the dunes.

Although N is the most active wind throughout the year (Fig. 2c), seasonal comparison of wind drift potential allows identification of two patterns: (1) spring–summer, when N (Polewards) winds are clearly prevalent, and (2) autumn–winter, when continental W and S (Equatorwards) winds are stronger. The directional variability of the wind regime, characterised by the RDP/DP ratio, shows intermediate values (0.39) i.e. between complex and bimodal patterns (Fryberger, 1979). In the study area, the bimodal pattern is clearly defined by north and south-west winds.

3.2. Dune morphology

Three dunefields are clearly distinguishable: the smaller one (NW) is on the north-west coast of the study area; the second, and largest one (WE), in the central area of the southern part of the peninsula forming a belt that stretches from west to east, from the Nuevo Gulf to the open Atlantic coast, and the third one (SW), also a fringe-like dunefield, in the south-west corner (Fig. 1). The three dunefields cover an area of approximately 884 km^2 and consist principally of 42 active dune megapatches, with a total area of 59 km^2, covering 7% of the southern portion of the Valdes Peninsula.

The NW dunefield constitutes a small area of 22 km^2 with 6 discrete dune megapatches (266 ha in total). The WE dunefield comprises a total area of 551 km^2, which includes 24 discrete megapatches located as far as 41 km away from the coast where they originated. The active dunes comprise an elliptically shaped mass, with

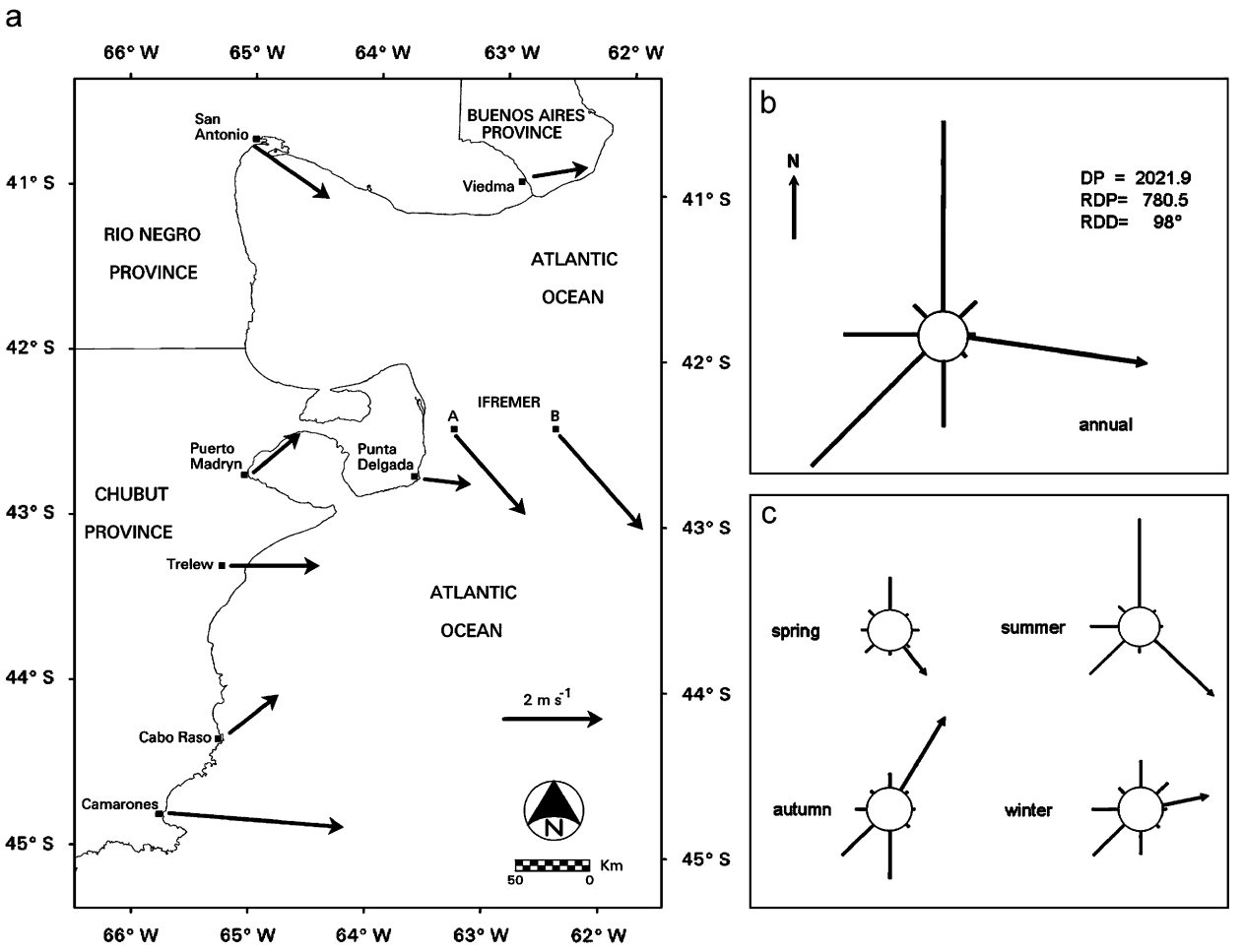

Fig. 2. (a) Regional annual wind regime: resulting vectors of wind intensity in north-eastern Patagonia. North wind intensity increases eastwards on the latitudes of the Valdes Peninsula. West component is overwhelmingly prevalent throughout the area. (b)–(c). Sand drift potential from vectorial analyses of the wind data in Punta Delgada station, following Fryberger (1979). (b) Rose diagram of annual drift potential (DP) in 8 wind direction sectors, the resultant drift potential vector (RDP) aligned in the resultant drift direction (RDD). (c) Seasonal wind regime as above: spring (September–November), summer (December–February), autumn (March–May) and winter (June–August).

its long axis in a north–north-easterly direction, covering a total surface of 4868 ha (mean megapatch area: 512 ± 264 ha). The bow-shaped fronts of dunes vary from 1 to 10 km in length. The SW dunefield covers a total area of 120 km^2 and includes 12 discrete megapatches. The active dunes' total area is 783 ha (mean megapatch area: 142 ± 94 ha). The bow-shaped fronts of dunes vary from 0.3 to 2.9 km in length.

Four main types of active sand dune forms were identified: (1) compound linear; (2) compound transverse; (3) compound dome-shaped; and (4) complex dome-shaped. Besides these dominant forms, a few scattered parabolic dunes, barchans, sand sheets and shrub dunes are also present in the area.

Compound linear dunes (7–13 m high) are located in the coastal NW dunefield (Appendix 1a–b, electronic version). Most linear dunes along the escarpment adopt a compound form owing to the NNE winds (Appendix 1b), attached to the cliff headland. A characteristic of linear dunes is that adjoining ridges often branch or merge at a "Y" junction. In the study area, junctions are most common where the ridge deflection occurs.

Compound transverse dunes (7–15 m high) are concentrated mainly in the W coast. The average trend of the dunes in this area is SE. The height of the dunes increases as the morphology becomes more intricate. Network dunes result from the intersection of transverse elements, where star-shaped dunes are also present.

Compound dome-shaped dunes (2–20 m high) occur in a wide area mainly in the WE and SW dunefields. Transverse sand ridges are locally superimposed on the domes and may modify them greatly (Appendix 2a–b, electronic version); the resulting dune form is transverse domal-ridge (row of connected domes). Barchanoid dunes and intergrading subtypes—small barchans (<3-m high) and mesobarchans (3–8 m high)—are also present. The barchan dunes occur as a solitary or as a compound type.

Complex dome-shaped dunes (4–20 m high) are located exclusively in the WE dunefield (Fig. 3). Transverse ridges and star dunes coalesce or grow together. Network dunes consist of NW–SE trending main ridges and nearly vertical secondary ridges (NE–SW orientation). In the interdunes areas among the dome dunes, there are also some sand ridges, small barchans, sparse mesobarchans and shrub dunes.

Within the three dunefields, stabilised discontinuous thin aeolian mantles are present, covering a total surface of about of 191 km^2. A well-developed vegetation cover of grasses (mainly *Sporobolus rigens*) and shrubs (principally *Hyalis argentea*) occurs on the dormant vegetated dunes with a very subdued topography. Local relief shows an undulating appearance and some of the depressions may reach the substratum (tertiary marine sediments or gravel deposits) upon which the dunefields lay.

Stabilised linear forms are much clearer in the northern and eastern sectors of the study area, but appear smoothed towards the inner part, among the megapatches. Westwards, these forms are strongly modified and show a superimposed younger morphology, resulting in a more complex pattern. These aeolian landforms seem to have been originally related to the development of parabolic and linear ridge dunes. The trends of the stabilised linear ridges suggest that they were formed by north and south-west winds.

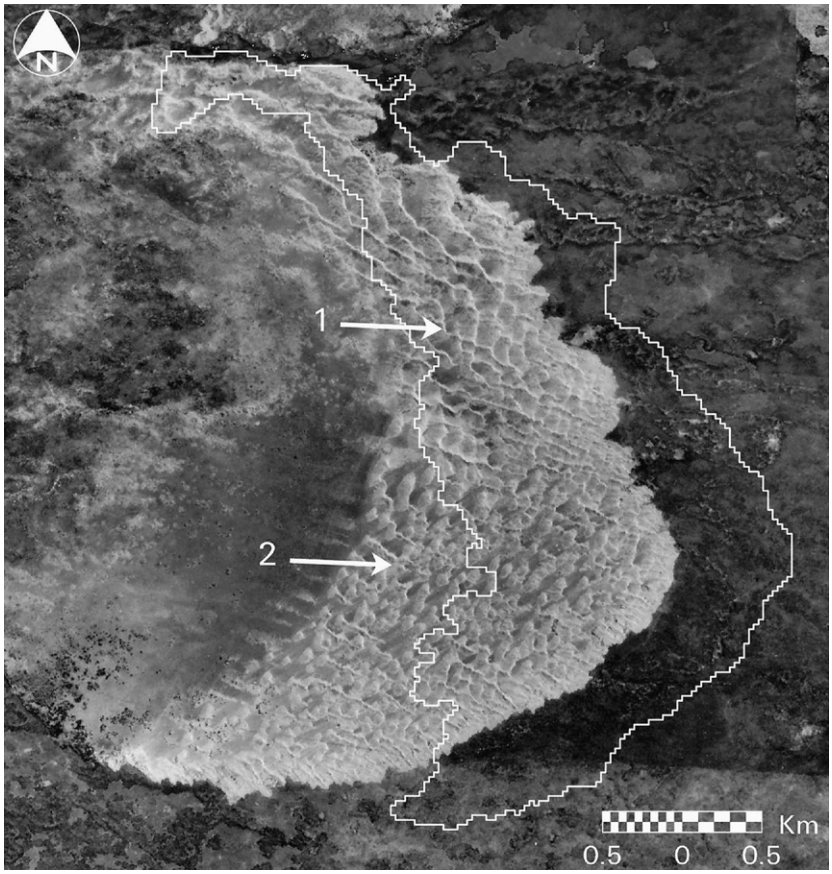

Fig. 3. Aerial photograph (7th January 1969). Complex dome-shaped dunes (megapatch 8, WE dunefield). Transverse ridges and star dunes coalesce or grow together (1). Note the dome, transverse and transverse domal ridges dunes (2). It can be seen that the complex dome shaped has changed its form mainly in the south part. The white polygon represents the dune megapatch boundaries digitised on Landsat image (7th February 2002).

3.3. Dune migration

The annual migration rate of the 30 dune megapatches was $9.1 \pm 2.7\,m\,yr^{-1}$ in the whole study period (1969–2002). Average rates were $8.1 \pm 2.4\,m\,yr^{-1}$ and $10.2 \pm 3.2\,m\,yr^{-1}$ in the periods 1969–1986 and 1986–2002, respectively. Annual rate (1969–2002) was $8.7 \pm 1.5\,m\,yr^{-1}$ in the NW dunefield, $8.8 \pm 2.8\,m\,yr^{-1}$ in the WE dunefield and $9.7 \pm 2.6\,m\,yr^{-1}$ in the SW dunefield. Total migration (in metres) during the study periods is shown in Fig. 4a.

The trend of the displacement of all the megapatches resulted in a drift direction (RDD) from W–NW. The azimuth of the displacement in the dunefields for the period of 1969–2002 were 121°, 107° and 119° for the NW, WE and SW dunefields respectively, quite in agreement with the RDD calculated by the Fryberger model. Taking the 30 sand dune megapatches as a whole, the azimuth was almost identical in the 1969–1986 (112.1°) and in the 1986–2002 (112.8°) periods.

The mean areas of the dune megapatches are different for the three dunefields identified in this study. Megapatches in the WE dunefield have a mean area of 4666 ± 124 ha, whereas in the NW and SW dunefields,

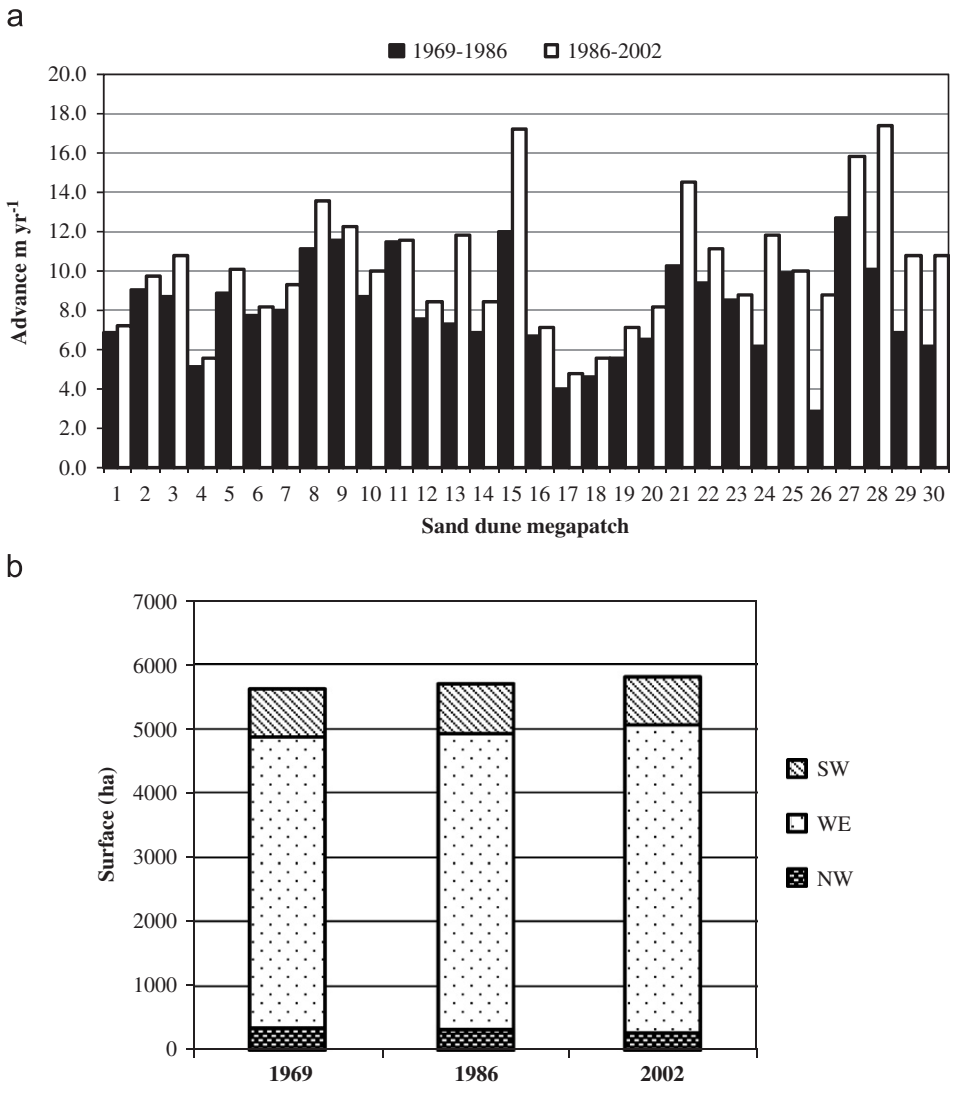

Fig. 4. (a) Advance $m\,yr^{-1}$ of active sand dune megapatch. (b) Surface of active sand dune megapatch (in hectares).

Table 2
Average values of main climatic variables within the considered periods

Period	Months	Mean dune migration ($m\,yr^{-1}$)	Mean wind speed ($m\,s^{-1}$)	% wind speed ($>4.5\,m\,s^{-1}$)	Rainfall (mm)		P PET^{-1}	Lancaster index (M)
					Total	Month		
1969–1986	214	8.1 ± 2.4	4.5	37.2	3374	15.8	0.20	186
1986–2002	183	10.2 ± 3.2	4.9	41.6	3064	16.7	0.18	231
1969–2002	397	9.1 ± 2.7	4.7	39.3	6438	16.2	0.19	207

PET: potential evapotranspiration (Thornthwaite and Mather, 1957).

the mean areas are 308 ± 26 and 771 ± 30 ha, respectively. The average area of the megapatches changed within the study period, showing a slightly decreasing trend in the NW and SW dunefields (−63 and −7 ha, respectively) and increasing trend in the WE dunefield (+260 ha). Despite these results, when changes are expressed in percentages of the total surface involved, megapatches of the WE dunefield appear as the most stable because of their greater area.

Considering the whole study area, the total surface of active dunes rose steadily from 5623 ha in 1969 to 5681 ha in 1999 and 5813 ha in 2002 (Fig. 4b). The final increase of 190 ha is exclusively due to the WE dunefield, whose positive rate conceals the negative ones in the smaller other dunefields. In short, changes in the total surface are small ($\pm 3\%$) considering the 33 years involved.

Like most arid lands, the climate of the study area shows an irregular alternating of arid and humid cycles and interannual variation of rainfall is very high. Changes may be as swift as 300% from one year to the following. Nevertheless, the 10-year running average allows identification of trends within the studied periods. During the period of 1969–1986, rainfall of most of the years was above the average, but the following period (1986–2002) showed the reverse situation despite the peak in 1992. The long-term average shows a clear decreasing trend from 1979 to 1995; the total rainfall was 10% greater in the first period (3374 mm versus 3064 mm).

Table 2 summarises climatic variables, dune migration and Lancaster index for the periods considered in this study. According to these results, dunes should be categorised as *flank active* in the period of 1969–1986 and *fully active* in 1986–2002, while for the whole study period they are very near the border between both categories.

4. Discussion and conclusions

4.1. Dune morphology

The dune types of the Valdes Peninsula are far from showing a simple pattern, regardless of the sector in which they are located. Dome-like dunes have long been considered embryonic forms that evolve into barchanoid types (Swinehart, 1990). The examples of compound and complex domes found in the Valdes Peninsula are closely spaced, coalescing mounds of sand with barchanoid ridges on their broad summits. Their outlines and topography suggest that many of these dome-like dunes could have originally been barchan dunes later modified by changes in wind regime (Swinehart, 1990). It is also possible that barchans merge into wave-like shapes to produce barchanoid ridges (Cooke et al., 1993) or transform into transverse dunes when a greater sand supply is available (Saqqa and Atallah, 2004; Wasson and Hyde, 1983).

In the western part of the study area, star dunes are sporadically distributed on the top of transverse dunes. These dune types develop mostly through the accumulation of sand from transverse dunes into areas of very changing wind direction (Lancaster, 1999). There appears to be little net movement of these dunes as response to aeolian activity and dune surface changes prevail instead of major positional shifts.

Studies of variations in dune types and patterns in a variety of dunefields indicate that dunes of different types can exist side by side even within relatively uniform wind regimes, whether there are either

topographic-induced modification of air flow or dunes of different ages (Lancaster, 1995). The general orientation of the dunefields in southern Valdes peninsula is in agreement with the regional wind flow from the WNW, and active dunes show a coincident trend. Notwithstanding, active dunes present a variety of forms—as described in this paper—which reflect local variations in the wind flow. In the area of this study, mesoscale wind circulation is strongly influenced by the shape of the coastline and the actual existence of the dunefields is due to this friable windward coast found nowhere else in Patagonia.

There have been no final conclusions for the period when the dunes and their morphology developed as the age of the desert has not been studied systematically. For the future, emphasis should be placed on detailed geomorphic and stratigraphic studies of dormant and relic dunes.

4.2. Wind patterns related to dune migration

According to its latitudinal location, the Valdes Peninsula (42°–42°50′S) falls within the planetary belt of the westerly winds, which in Patagonia are kept in motion by the South Pacific high-pressure centre and the sub-polar low-pressure trough (Prohaska, 1976); although the west component prevails throughout the vast area south 40°S, regional variations exist.

In the western stations, close to the Andean range, the west wind is overwhelmingly prevailing, while eastwards, on the Atlantic shore, an increasing of SW and NW frequencies are noticeable. This modification in the general flux from the west stems from the low-pressure cells detached from the sub-polar trough, migrating northwards up to 45°S approximately, which in the north-eastern Patagonian region determine a change in wind direction from SW to W and then to NW. This occurs quite often, so as to become visible in the records.

Further east, this cyclonic circulation blends with the one of the Atlantic high-pressure centres. Depending on the shift of this centre, maritime air masses from N or NE can invade NE Patagonia. Roughly, it can be said that over the general circulation from the west, minor topographic-induced circulations overlap, as well as synoptic circulations regionally modified.

The average orientation of dunefields in the south sector of the Valdes Peninsula agrees to this macro-scale atmospheric circulation, which has been active at least since the beginning of the Holocene (Haller et al., 2000). The average direction of the displacement of all the dunes taken as a whole is 112°, which indicates an increase in the N component of wind as compared to stations located westwards, such as Puerto Madryn (80-km W) or Trelew (100-km WSW). North-west winds do not prevail in any of them, but they become predominant in stations further north or north-east (Viedma 225-km NE, or San Antonio 240-km NNW).

Remote assessment of wind speed and direction on the ocean close to the Valdes Peninsula confirms the rising of the meridian component in circulation while moving eastwards. Atmospheric circulation in Points A and B, respectively, located 60- and 135-km ENE from the study area, shows a different pattern compared to stations located an equivalent distance westwards, where south-west and west winds prevail. The orientation of the dunefields in the Valdes Peninsula (WNW–ESE) responds to intermediate conditions in wind direction, between the west wind prevailing towards the west and the north wind prevailing towards the east, according to a mid-way geographic location.

The inland dunes are attributed to a receptive shoreline, backed by flat topography leeward, upon which dune migration is facilitated. These conditions are found in the southern sector of the Valdes Peninsula but not in the northern sector, owing to differences in the shoreline height. We could summarise the apparent histories of dune displacement and reactivation for each megapatch studied. It is clear that the dune migration takes place into established vegetation.

Because of the windy climate of the study area, sand dune megapatches in the Valdes Peninsula show some of the highest drift rates as compared to coastal or continental dune systems (Barbosa and Domínguez, 2004; Muhs and Wolfe, 1999; Tsoar and Blumberg, 2002). The sand dunes may migrate faster if they coalesce, as it usually occurs in these megapatches; wavy forms and ample sand supply produce wind entrainment and difficult vegetation growth that impede saltation. Besides, less near-surface obstruction facilitates laminar flow, downwind transport of sand and sustained flow towards the dune crest, enhancing migration (Marin et al., 2005).

According to Hugenholtz and Wolfe (2005), historical dune activity reflects the balance between two major geomorphic changes to the landscape: (1) dune migration and reactivation of stabilised surfaces, which increase the active area, and (2) vegetation encroachment, which reduces the area of active sand.

Examination of the dune megapatch displacement shows that the tempo of dune stabilisation was not synchronous among dunefields. For example, there was a declining trend in the rate of stabilisation at the WE dunefield, whereas increasing trends occurred at the NW and SW dune fields. At the same time, some of the megapatches of the WE dunefield showed a very clear stabilisation. This means that some megapatches have a singular behaviour that may be quite different to the general trend of the corresponding dunefield. These singularities might be due to grazing management effects, which vary between paddocks (Blanco, 2004). Besides, the apparent stabilisation of megapatches of the SW dunefield is not strictly true, since the net decrease of the active dune area is not due to the vegetation gaining ground but to the loss of sand blowing to the sea in megapatches located on the cliff, at the end of the cycle.

Mean displacement rate of dune megapatches is lesser in the NW dunefield than in the two others. This dunefield is at the west cost of the Valdes Peninsula, where the Points Pirámides and Pardelas create some wind shadow to the prevailing WNW winds. On the other hand, inland topography is not the same as that of the other dunefields, as immediately eastwards there is a relative depression that retains aeolian sediments and perturbs normal wind flow.

Based on the pattern of the active megapatches of the Valdes Peninsula, the orientation of the dunes has not changed significantly over 33 years. The azimuth of the displacement of the dunes was not the same in the three dunefields since it was significantly lower in the WE dunefield related to the NW and SW ones.

These observations lend support to the argument that dune mobility primarily reflects the interactions of two factors. Firstly, the degree of windiness, expressed as wind speed exceeding the threshold, or as the percentage of days with winds above the threshold of sand movement (Tsoar, 1989; Tsoar and Blumberg, 2002). Secondly, the effective annual precipitation, as a driving factor of vegetation growth or decline. The vegetation cover can be a major determinant in modifying wind flow and trapping sediment on dune surfaces (Wiggs et al., 1995; Wolfe, 1997).

Acknowledgements

We wish to acknowledge the valuable observations made to this work by the anonymous reviewers. Also, we are grateful to Dr. Alfred Zinck (International Institute for Geo-Information Science and Earth Observation, Enschede, Netherlands) who has helped to improve this manuscript. This research was funded by the following projects of Argentina: PIP 02127 and 6413 (CONICET), PICT98-07-04094 (FONCyT) and BID 1201/OC-AR-PICTR 2003-439. Funding from CONAE (“Comisión Nacional de Actividades Espaciales”) or the Argentinean Space Agency was also devoted to this research to promote monitoring of World Heritage sites (UNESCO). The Global Land Cover Facility (GLCF) of the University of Maryland provided scenes of Landsat (March 27, 1976 and November 2, 1986). Thanks are given to G. Zar and W. Tretter for technical comments and assistance.

Appendix A. Supplementary data

Supplementary data associated with this article can be found in the online version at doi:10.1016/j.jaridenv.2007.07.011.

References

Bannari, A., Morin, D., Benie, G.B., Bonn, F.J., 1995. A theoretical review of different mathematical models of geometric corrections applied to remote sensing images. Remote Sensing Reviews 13, 27–47.

Barbosa, I.M., Domínguez, J.M.L., 2004. Coastal dune fields at the Sao Francisco River strandplain, northeastern Brazil: morphology and environmental controls. Earth Surface Processes and Landforms 29 (4), 443–456.

Bishop, S.R., Momiji, H., Carretero-González, R., Warren, A., 2002. Modelling desert dune fields based on discrete dynamics. Discrete Dynamics in Nature and Society 7 (1), 7–17.

Blanco, P.D., 2004. Características morfológicas y dinámica de los focos de deflación de los pastizales naturales del suroeste de Península Valdés (Chubut). Thesis, Licenciatura en Biología. Universidad Nacional de la Patagonia San Juan Bosco (UNPSJB), Sede Puerto Madryn (Chubut), Argentina, 87pp.

Bouza, P.J., Simón Torres, M., Rostagno, C.M., Aguilar Ruiz, J., del Valle H.F., 2002. Propiedades físicas, químicas y mineralógicas de aridisoles en península Valdés. XVIII Congreso Argentino de la Ciencia del Suelo, Puerto Madryn (Chubut), 16–19 April 2002, CD-ROM, 8pp.

Bouza, P., Simón Torres, M., Aguilar Ruiz, J., Rostagno, C.M., del Valle, H.F., 2005. Genesis of some selected soils in the Valdes Peninsula NE Patagonia Argentina. In: Faz Cano, A., Ortiz, R., Mermut, A. (Eds.), Advances in Geoecology 36: Genesis, Classification and Cartography of Soils. Catena Verlag GMBH, Germany, pp. 1–12 (chapter 1).

Collado, A.D., Chuvieco, E., Camarasa, A., 2002. Satellite remote sensing analysis to monitor desertification processes in the crop-rangeland boundary of Argentina. Journal of Arid Environments 52, 121–133.

Cooke, R., Warren, A., Goudie, A., 1993. Desert Geomorphology. UCL Press, London.

ERDAS Inc., 2003. ERDAS, versión 8.7. 〈http://www.erdas.com/〉.

Fryberger, S.G., 1979. Dune forms and wind regime. In: McKee Edwin, D. (Ed.), A Study of Global Sand Seas Geological Survey Professional Paper, vol. 1052. United States Geological Survey, Washington, DC, pp. 137–169.

Haller, M.J., Monti, A.J., Meister, C.M., 2000. Hoja Geológica 4363-I: Península Valdés, Provincia del Chubut. Programa Nacional de Cartas Geológicas de la República Argentina, 1:250000. Boletín No 266, Servicio Geológico Minero Argentino, Buenos Aires, Argentina.

Hugenholtz, C.H., Wolfe, S.A., 2005. Recent stabilization of active sand dunes on the Canadian prairies and relation to recent climate variations. Geomorphology 68, 131–147.

Janke, J.R., 2002. An analysis of the current stability of the Dune Field at Great Sand Dunes National Monument using temporal TM imagery (1984–1998). Remote Sensing of Environment 83, 488–497.

Lancaster, N., 1988. Development of linear dunes in the southwestern Kalahari, Southern Africa. Journal of Arid Environments 14, 233–244.

Lancaster, N., 1995. Origin of the Gran Desierto sand sea, Sonora, Mexico: evidence from dune morphology and sedimentology. In: Tchakerian, V. (Ed.), Desert Aeolian Processes. Chapman & Hall, London, pp. 11–35.

Lancaster, N., 1999. Geomorphology of desert sand seas. In: Goudie, A.S., Livingstone, I., Stokes, S. (Eds.), Aeolian Environments, Sediments and Landforms. Wiley, Chichester, pp. 49–70.

León, R.J.C., Bran, D., Collantes, M., Paruelo, J.M., Soriano, A., 1998. Grandes unidades de vegetación de la Patagonia extrandina. Ecología Austral 8 (2), 275–308.

Levin, N., Ben-Dor, E., 2004. Monitoring sand dune stabilization along the coastal dunes of Ashdod-Nizanim, Israel, 1945–1999. Journal of Arid Environments 58, 335–355.

Marin, L., Forman, S.L., Valdez, A., Bunch, F., 2005. Twentieth century dune migration at the Great Sand Dunes National Park and Preserve, Colorado, relation to drought variability. Geomorphology 70, 163–183.

McKee, E.D., 1979. Introduction to a study of global sand seas. In: McKee, E.D. (Ed.), A Study of Global Sand Seas. USGS Professional Paper, 1052, USA, pp. 1–19.

Muhs, D.R., Wolfe, S.A., 1999. Sand dunes of the northern Great Plains of Canada and the United States. In: Lemmen, D.S., Vance R.E. (Eds.), Holocene Climate and Environmental Change in the Palliser Triangle, Bulletin, 534, Geological Survey of Canada, pp. 183–197.

Paisley, E.C.I., Lancaster, N., Gaddis, L.R., Greelye, R., 1991. Discrimination of active and inactive sand from remote sensing: Kelso Dunes, Mojave Desert, California. Remote Sensing of Environment 37, 153–166.

Paruelo, J.M., Beltrán, A.B., Jobbágy, E.G., Sala, O.E., Golluscio, R.A., 1998. The climate of Patagonia: general patterns controls on biotic processes. Ecología Austral 8, 85–101.

Peuquet, D.J., 1981. An examination of techniques for reformatting cartographic data part 1: the raster to vector process. Cartographica 18 (1), 34–48.

Prohaska, F., 1976. The climate of Argentina Paraguay and Uruguay. In: Schwerdtfeger, W. (Ed.), The Climate of Central and South America. World Survey of Climatology. Elsevier, New York, pp. 13–143.

Saqqa, W., Atallah, M., 2004. Characterization of the Aeolian terrain facies in Wadi Araba Desert southwestern Jordan. Geomorphology 62, 63–87.

Súnico, A., 1996. Geología del Cuaternario y Ciencia del Suelo: relaciones geomórficas-estratigráficas con suelos y paleosuelos. Doctoral Thesis, Facultad de Ciencias Exactas y Naturales, Departamento de Graduados, Universidad Nacional de Buenos Aires (UBA), 227pp.

Swinehart, J.B., 1990. Wind-blown deposits. In: Bleed, A., Flowerday, C. (Eds.), An Atlas of the Sand Hills, Resource Atlas No. 5a. Conservation and Survey Division, Inst. Agriculture and Natural Resources, University of Nebraska-Lincoln, pp. 43–56.

Thornthwaite, C.W., Mather, J.R., 1957. Instructions and tables for computing potential evapotranspiration and the water balance. Publications in Climatology (Laboratory of Climatology, Centertown, NJ) 10, 185–311.

Tsoar, H., 1989. Linear dunes—forms and formation. Progress in Physical Geography 13 (4), 507–528.

Tsoar, H., Blumberg, D.G., 2002. Formation of parabolic dunes from barchan and transverse dunes along Israel's Mediterranean coast. Earth Surface Processes and Landforms 27 (11), 1147–1161.

Wasson, R.J., Hyde, R., 1983. Factors determining desert dune type. Nature 304, 337–339.

Wiggs, G.F.S., Thomas, D.S.G., Bullard, J.E., Livingstone, I., 1995. Dune mobility and vegetation cover in the southwest Kalahari Desert. Earth Surface Processes and Landforms 20, 515–530.

Wolfe, S.A., 1997. Impact of increased aridity on sand dune activity in the Canadian Prairies. Journal of Arid Environments 36, 421–432.